

Enhancement of surface hardness and metallurgical properties of AISI 410 by laser hardening process; diode and Nd:YAG lasers

Moradi, M., Arabi, H., Karami Moghadam, M. & Benyounis, K. Y.

Author post-print (accepted) deposited by Coventry University's Repository

Original citation & hyperlink:

Moradi, M, Arabi, H, Karami Moghadam, M & Benyounis, KY 2019, 'Enhancement of surface hardness and metallurgical properties of AISI 410 by laser hardening process; diode and Nd:YAG lasers', *Optik*, vol. 188, pp. 277-286.

<https://dx.doi.org/10.1016/j.ijleo.2019.05.057>

DOI 10.1016/j.ijleo.2019.05.057

ISSN 0030-4026

Publisher: Elsevier

NOTICE: this is the author's version of a work that was accepted for publication in *Optik*. Changes resulting from the publishing process, such as peer review, editing, corrections, structural formatting, and other quality control mechanisms may not be reflected in this document. Changes may have been made to this work since it was submitted for publication. A definitive version was subsequently published in *Optik*, 188, (2019) DOI: 10.1016/j.ijleo.2019.05.057

© 2019, Elsevier. Licensed under the Creative Commons Attribution-NonCommercial-NoDerivatives 4.0 International

<http://creativecommons.org/licenses/by-nc-nd/4.0/>

Copyright © and Moral Rights are retained by the author(s) and/ or other copyright owners. A copy can be downloaded for personal non-commercial research or study, without prior permission or charge. This item cannot be reproduced or quoted extensively from without first obtaining permission in writing from the copyright holder(s). The content must not be changed in any way or sold commercially in any format or medium without the formal permission of the copyright holders.

This document is the author's post-print version, incorporating any revisions agreed during the peer-review process. Some differences between the published version and this version may remain and you are advised to consult the published version if you wish to cite from it.

Enhancement of Surface Hardness and Metallurgical Properties of AISI 410 by Laser Hardening Process; Diode and Nd:YAG Lasers

Mahmoud Moradi^{1,2*}, Hossein Arabi^{1,2}, Mojtaba Karami Moghadam^{1,2}, Khaled Y. Benyounis³

1-Department of Mechanical Engineering, Faculty of Engineering, Malayer University, Malayer, Iran

2-Laser Materials Processing Research Center, Malayer University, Malayer, Iran

3- School of Mech. & Maun. Eng., Dublin City University, Dublin, Ireland

Abstract:

This paper investigates the experimental study of laser surface hardening (LSH) of AISI 410 martensitic stainless steel by using two industrial lasers; 1600 W high power diode laser and 700 W Nd:YAG laser. The influence of the distribution and shape of the laser beam; Top-hat in diode laser and Gaussian distribution in Nd:YAG laser, have been investigated on the micro-hardness, geometrical dimensions of the hardened area (depth and width), microhardness deviation (MHD) from the base metal in width and depth of hardened layer, and the ferrite phase percentage. Microstructure evaluation of the laser hardened zones were performed using optical and FE-SEM. Results show that the diode laser creates a higher surface hardness, more depth and width of hardness, more MHD in depth and width and less ferrite phase than the Nd:YAG laser, which is because of lower wavelength of diode laser (808 nm) than Nd:YAG laser (1064 nm) that lead to higher laser energy absorption. Observations indicate that hardened layer of diode laser is about 620 HV0.3 with 1.8 mm depth, while for Nd:YAG laser is about 598 HV0.3 with 0.211 mm depth.

Keywords: Laser Surface Hardening; Diode Laser; Nd:YAG laser; AISI 410 martensitic stainless steel; Micro hardness

1. Introduction

LSH is one of the important and modern industrial processes which apply high energy density of the laser beam with very rapid heat on the surface of the workpiece at above the austenitic temperature of the steel [1]. The thermal energy absorbed by the surface layer is quickly distributed into the workpiece. This heat diffusion results in a very rapid temperature drop in the hardened area [2]. High cooling gradient has resulted in a fine-grained martensitic structure with very high hardness, which is the major advantage compared with conventional methods of hardening [3]. Figure 1, illustrates the schematic of the laser hardening process.

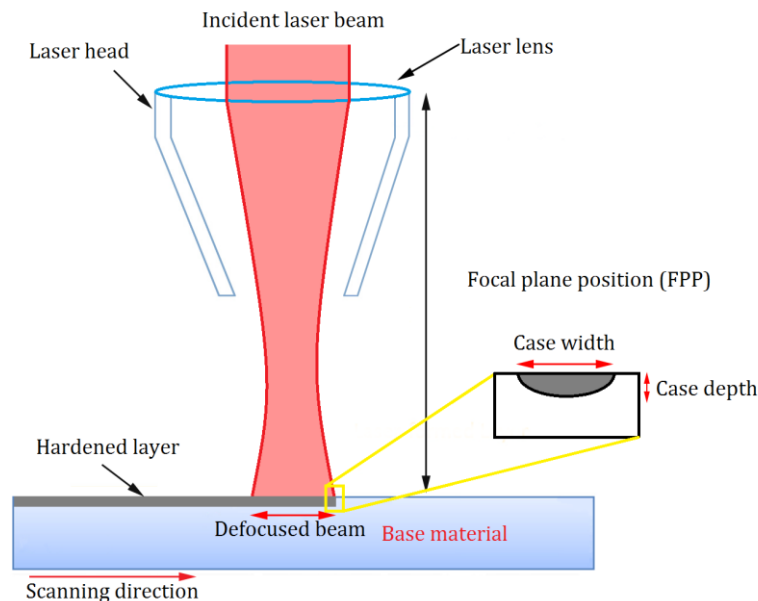


Figure 1. Schematic of the laser hardening process [4]

In the laser hardening, after the cooling process, the martensitic phase will be formed. In this method, less distortion occurs compared with induction and flame methods [5]. Due to the numerous advantages of lasers in industries, they are widely used in different applications such as; laser welding and LSH [6-11], laser cutting and drilling [12-14] which are called laser materials processing.

In 1997, Klocke et al. [15] performed diode LSH with power of 650 W on 42CrMo4 steel. The purpose of this study was to increase the beam intensity of the diode laser by considering laser input parameters. The hardness of steel was reach to 700 HV with depth of 0.5 mm. Haug et al. [16] in 1997, by using a diode laser with 300 W power studied on the LSH process of the 100Cr6 steel to increase the hardness to 850 HV with 0.45 mm depth. Pantelis et al. Also, Wear of hardened area [17], triabiological properties [18] and simulation of the LSH [19] were investigated in other researches. Ehlers et al. [20] carried out LSH of AISI 4140 steel by using a 2 kW diode laser to achieve the maximum hardness of 740 HV and 1.9 mm depth. Moradi et al. [21] conducted a study on the LSH of AISI 410 steel by using Nd:YAG laser. Benyounis et al. [22] in 2016, carried out a research in association with the nitrogen gas coating on the 316L, 316 and 304 stainless steel on the basis of the design of

the experiments method. Li et al. investigated a research on the LSH of AISI 1045 by using two types of laser; high- power diode laser and a CO₂ laser. The result showed that rectangular laser beam with uniform energy distribution in diode laser is more applicable and effective than circular laser beam with Gaussian distribution energy in CO₂ laser [23]. Fahdil iidan et al. [24] studied a comparative analysis of hardness after hardening, hardening & tempering, and CO₂ laser hardening on 40, 40Cr and 38Cr2MoAl steels in GOST Russian standard. Saftar et al. [25] investigated the effects of beam geometries (circular, inverse triangle, rectangular beams) by using high power diode laser on the LSH process. Moradi et al. [26] carried out a study on the diode laser hardening process of AISI 410 by using RSM method. Jahromi et al. [27] investigated a study by Nd:YAG laser on the three different microstructures of AISI 410 martensitic stainless steel samples were heat treated including: fine ferrite, fine and coarse martensite.

Effects of the LSH by using these two types of laser is investigated on the hardening characteristics; the geometric dimensions of the hardened area (depth and width), the microhardness distribution, the micro hardness deviation from the base metal micro hardness (MHD), the microstructure, and the percentage of the ferrite phase in the structure of the hardened area. The results of laser hardening processes are compared with furnace hardening heat treatment.

2. Experimental Work

Material used in this study is AISI 410 Martensitic stainless steel with the chemical composition mentioned in Table 1.

Table 1. Chemical composition (Wt. %) of AISI 410

Element Name	C	Mo	Cr	Cu	S	P	Mn	Ni	Si	Al	V	Fe
Weight percent	0.15	0.03	13.5	0.11	0.024	0.018	0.51	0.12	0.28	0.008	0.021	Balance

The LSH of AISI 410 was carried out with 1600 W diode and 700W Nd:YAG lasers. Table 2 and Table 3, show the settings and results of the laser hardening process of AISI 410 by using diode laser and Nd:YAG laser, respectively.

Table 2. Settings and results of the Diode laser hardening of AISI 410 (A1-A4)

Sample Number	Input parameters			Output results							
	Scanning speed (mm/s)	Focal plane position (mm)	Laser Power (w)	Heat Input (J/mm)	Depth of Hardness (mm)	Maximum Hardness (hv)	Width of Hardness (mm)	Ferrite percent (%)	MHD in width	MHD in depth	
A1	6	70	1600	266.6	1.8	620	8.3	0.5	18813.7	28651.6	
A2	5	65	1400	280	2.2	600	8.1	0.62	18658.42	26621.6	
A3	6	60	1200	200	2.2	520	8.1	1.5	15090.5	20074.5	
A4	5	65	1000	200	1.1	515	8.6	1.9	12711.89	16890.1	

Table 3. Settings and results of the Nd:YAG laser hardening of AISI 410 (B1- B4)

Sample Number	Input parameters					Output results						
	Scanning speed (mm/s)	Focal plane position (mm)	Mean power (W)	pulse Width (m s)	pulse Energy (J)	Heat Input (J/m)	Depth of Hardness (mm)	Maximum Hardness (h v)	Width of Hardness (mm)	Ferrite percent (%)	MHD in width	MHD in depth
B1	2	24	220	14	14.7	110	0.142	546	2.107	1.2	13200	15100
B2	2	24	236	15	15.75	118	0.211	598	2.188	0.85	15400	15400
B3	2.5	24	220	14	14.66	88	0.1250	365	1.805	3.1	9200	5100
B4	2.7	24	220	14	14.66	81.48	0.071	322	1.768	3.5	8400	4200

In samples cross-section, for each sample, micro hardness was measured by the micro-indentation device from the surface to the depth of laser penetration and also in width. For metallographic operations, the hardened cut specimens prepared by polishing and etching in the villa's reagent and prepared for microstructure analysis. The depth (h) and width (w) of the hardened area are shown in [Figures 2](#), for diode and Nd:YAG lasers, respectively.

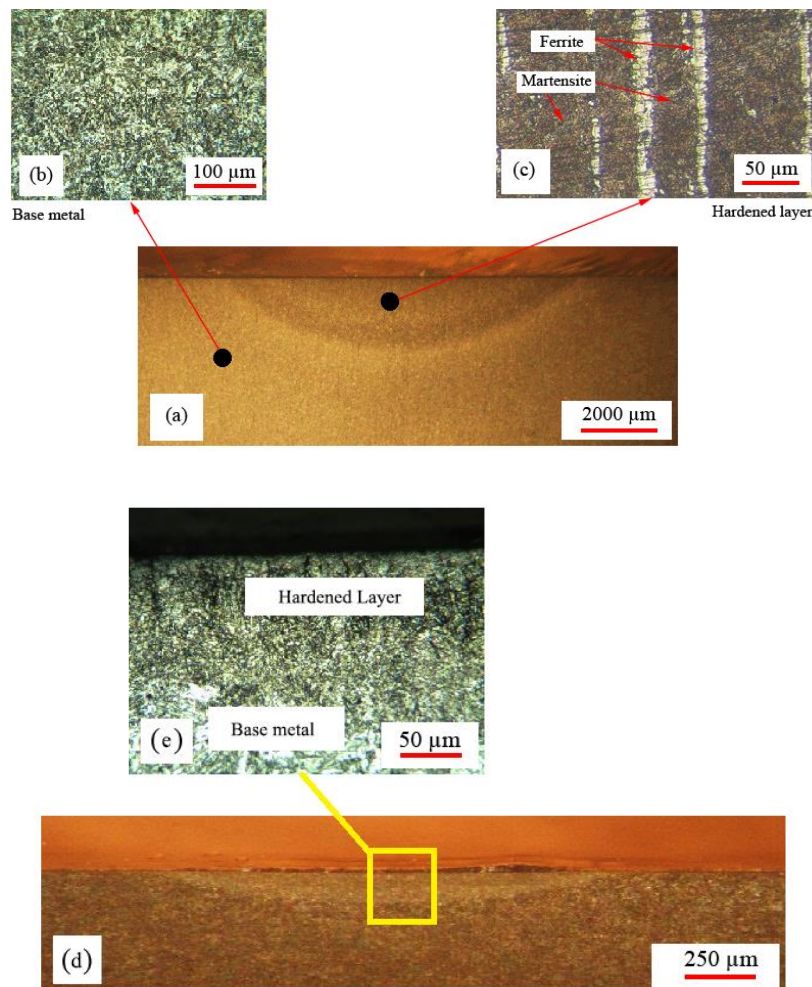


Figure 2. a) Cross section of the hardened sample of AISI 410 by using Diode laser b) Base metal of AISI 410 c) Hardened area from Diode LSH d) Cross section of the hardened sample of AISI 410 by using Nd:YAG laser e) Hardened area from Nd:YAG LSH

3. Investigate in Nd:YAG and Diode laser beam from LSH

In the present research, all conditions including the physical properties of steel, surface topography and the percentage of alloy elements in the basic chemical composition of the steel, are the same. The main difference in this study is the type of the laser beam. The wavelength of the laser and the shape of the laser energy distribution are the most important factors effect on the laser absorption to the material. The laser absorbed energy depends on many factors [28].

For opaque materials, the absorptivity (A) can be defined by Equation 1 [29]:

$$A=1-R \quad (1)$$

Where R is the material reflectivity which at normal incidence is defined by Equation 2:

$$R= [(1-n)^2+K^2]/ [(1+n)^2+K^2] \quad (2)$$

While parameters n and k are strong functions of wavelength and temperature, the reflectivity (and therefore the absorptivity) of the material is greatly influenced by the wavelength and temperature [29, 30].

Diode laser distribution is rectangular form in focal plane with dimension of 8 mm ×1.5 mm while for Nd:YAG laser is Gaussian with a spot cycle point with 0.4 mm diameter. In fact, the shape of the Nd:YAG laser beam is circular form and the shape of the diode laser beam is a rectangular in a slow direction is in the form of a Top-Hat and in the other fast direction is the form of a Gaussian [31-34].

4. Results and discussion

4-1 Microhardness distribution of hardened area

Figure 3 depicts trend of micro hardness changes from the surface to depth by using diode and Nd:YAG lasers for different AISI 410 samples. As shown in Figure 3, the maximum hardness of the hardened areas of A1 to A3 samples by diode laser is greater than of B1 to B3 samples by Nd:YAG laser.

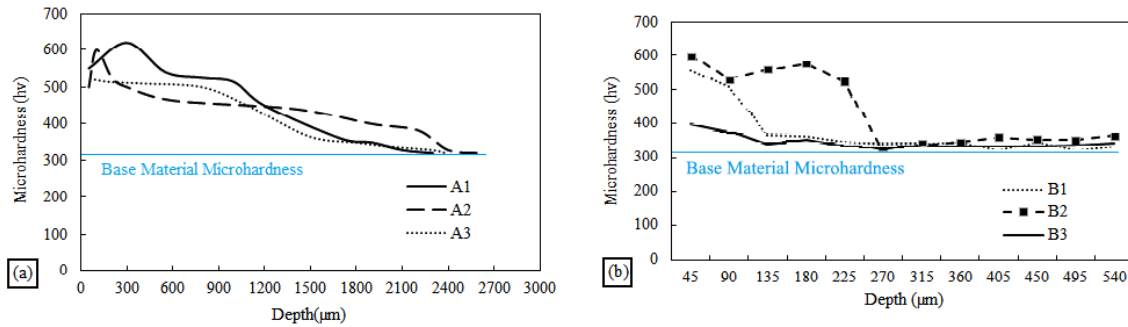


Figure 3. Micro hardness profile of the depth of hardened area of AISI 410 by using a) diode laser b) Nd:YAG laser

Figure 4 illustrates the changes in the micro hardness on the width of the hardened area from the center to the base metal. It is clear that the maximum hardness in the width of the hardened area will be achieved by using diode laser in the samples of A1 to A3 is more than the Nd:YAG laser in the samples of B1 to B3. Having higher heat input in diode laser than Nd:YAG laser, approximately two times (see Table 2 and 3), lead to higher hardness and depth.

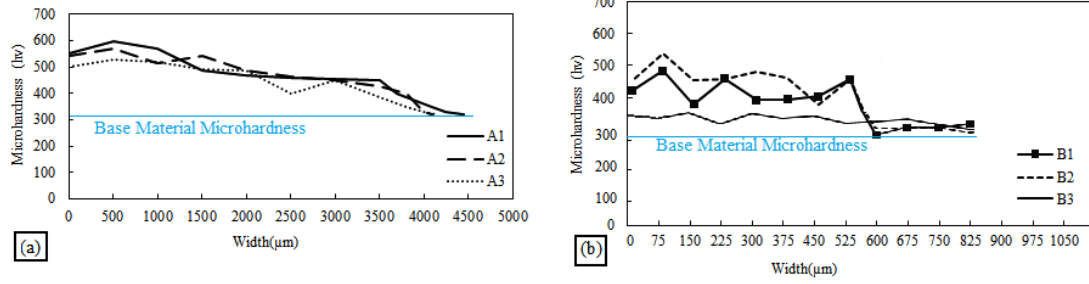


Figure 4. Micro hardness profile at the width of hardened area of AISI 410 by using diode laser (a) & Nd:YAG laser (b)

The surface hardness depends on two total factors, the heat input entering the workpiece, and the energy absorption. Heat input equation for laser materials processing is given in Equation 3 [12]:

$$HI = P/V \quad (3)$$

Where in Equation 3, HI is the heat input (j), P is laser power (w), V is scanning speed (mm/s). The calculated heat input is presented in Table 2 and 3.

In this study, the maximum heat input in hardened samples by using Diode and Nd:YAG lasers are 280 J/mm and 180 J/mm , respectively. By increasing the heat input to the workpiece surface, the austenitic temperature of the steel rises and more austenite particles are being created. Then, with the cooling the steel which known as a self-quenching mechanism, a more martensitic phase is created which increases the surface hardness of the steel.

Table 4 shows the physical properties of AISI 410 and Absorptivity percentage of diode and Nd:YAG lasers.

Table 4. Physical properties & Absorptivity percentage of AISI 410

Physical & thermal properties	Density, lbs/in ³ (g/cm ³)	Thermal Conductivity, BTU/hr/ft/(W/m/k)	Modulus of Elasticity, ksi. (Mpa)	Specific, Heat, BTU/lbs°F(kj/kg/k)	Absorptivity,% [28]	
					Nd:YAG laser	Diode laser
AISI410	7.74	24.9	200	0.46	28-31	45

As shown in Table 4, the absorption coefficient of diode and Nd:YAG lasers are 45% and 31%, respectively. Therefore, by increasing in the absorption of laser beam, more energy transfers to the material and less is reflected. The ASTM-112 standard is used to measure the grain size of particles in the microstructure of AISI 410 hardened samples. Knowing that the ferrite and martensite particles in the hardened microstructure of AISI 410 are extremely fine, at first, the initial austenitic grains are evaluated by performing a normalize heat treatment cycle on the hardened laser samples in the furnace. Then, with the criteria given in ASTM-112, the particle size is determined, finally, with respect to these particle sizes, the size of the particles in the microstructure of AISI 410 is estimated. In the present study, the grain size of the base metal according to ASTM standard is number 7 ($30\mu\text{m}$) which reach to ASTM grain size number 11 ($7 \mu\text{m}$) in the Diode laser hardening and ASTM grain size number 9 ($15 \mu\text{m}$) in the Nd:YAG laser hardening. According to the ASTM-112 standard, a higher ASTM grain size number results in a smaller hardened grain size. So, the diode laser hardening operation has a finer grain size and subsequently higher hardness than the Nd:YAG laser hardening

operation. The relationship between grain size and mechanical properties is expressed by the Hall-Petch equation [28]. Equation 4 explain this relation:

$$\sigma_0 = \sigma_i + KD^{-1/2} \quad (4)$$

Where σ_i is yield stress, σ_0 is the friction stress, K is the locking parameter and D is the mean diameter of the grain [35]. So, by increasing the hardness, the grain sizes reduce, and also the strength of the material and mechanical properties improve.

4-2 Geometrical dimensions of hardened layer (depth & width)

Figure 5 shows the geometrical dimensions (depth and depth) of the hardened area of AISI 410 by using a) diode and b) Nd:YAG laser.

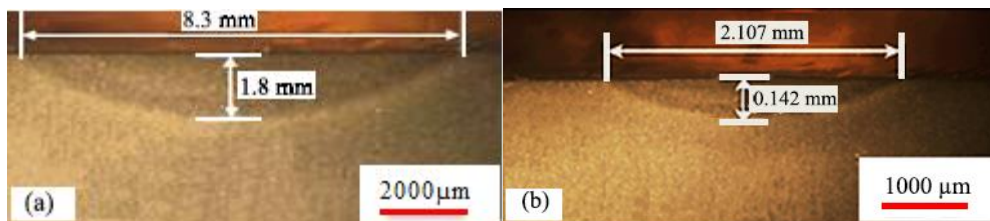


Figure 5. a) Cross section of geometric dimensions (depth and width) hardened area by using diode laser for sample A1 b) Cross section of geometric dimensions (depth and width) hardened area by using Nd:YAG laser for sample B1

The effective factors in increasing the geometrical dimensions of the hardened area in diode laser are the heat input and the laser beam distribution. As seen in Figure 5 diode laser cover a higher area of the material surface than the Nd:YAG laser. In both lasers, the center of the laser beam has more heat than the corners of the spot of the laser beam [36]. Figure 6 shows the micro hardness distribution in depth of hardened zone of AISI 410 by using Diode and Nd:YAG lasers.

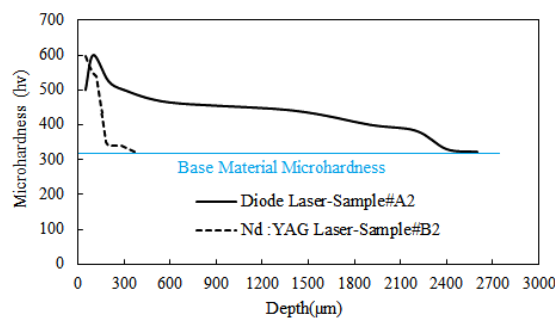


Figure 6. Micro hardness distribution in the depth of the hardened area of AISI410 by diode laser and Nd:YAG laser

As can be seen in Figure 6, the depth of penetration of the laser beam in the hardened area of AISI 410 by diode laser is higher than Nd:YAG laser. The rectangular distribution of laser beam energy in the diode laser makes the surface more exposed to thermal energy and has a higher penetration depth. Figure 7 shows the micro hardness distributions of hardened area in width of AISI 410 by using Diode and Nd:YAG lasers. As shown in Figure 7, it is clear that the width of the hardened area of AISI 410 by diode laser is greater than Nd:YAG laser.

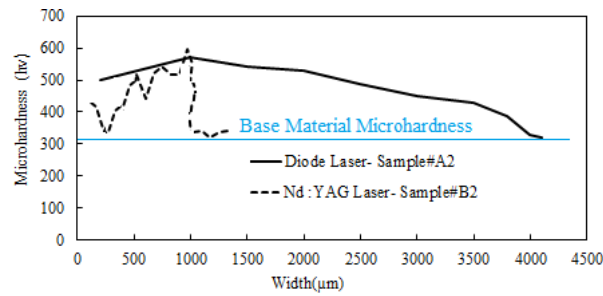


Figure 7. Micro hardness distributions in the hardened area in width of AISI 410 by diode and Nd:YAG lasers

4-3 Microstructure of hardened layer

The microstructure of AISI 410 of the base material is shown in [Figure 8](#), in which the ferrite particles are observed in the martensite field.

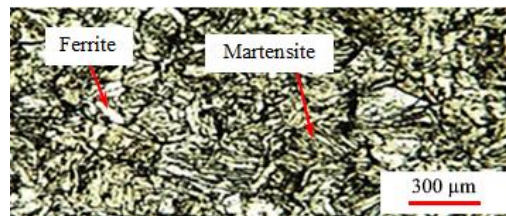


Figure 8. Microstructure of base metal of AISI 410

[Figure 9](#) depicts the hardened layer images and the microstructure of this layer hardened by diode and Nd:YAG lasers. It can be seen that the ferrite phase particles have been dispersed in the field of fine grain martensites. Due to the high speed of the cooling mechanism known as self-Quenching and the lack of enough time to dissolve ferrite particles, ferrite particles are solved incompletely and remains in the hardened structure [36]. Higher thermal input energy, causes the austenitic temperature rises to produce phase transformation and the ferrite grains become smaller. Due to the higher thermal energy and energy absorption in the diode laser (as explained in section 3), the percentage of ferrite particles in the martensite is reduced ([Figure 9-c and d](#)).

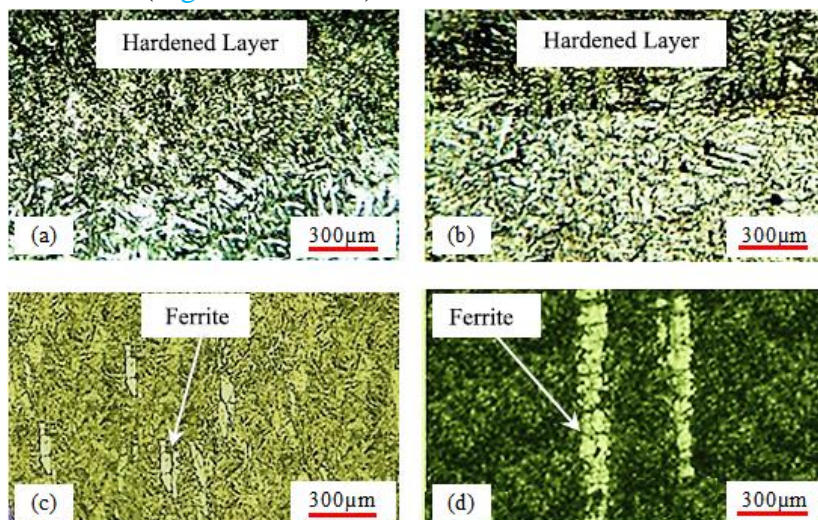


Figure 9. Images of a) hardened layer of diode laser, b) hardened layer of Nd:YAG laser, c) Microstructure of hardened layer of diode laser, d) Microstructure of hardened layer of Nd:YAG laser

Figure 10 illustrates the FESEM images of hardened layer and base metal of AISI 410. In the images of the FESEM microstructure, ferrite phase particles in the martensite field are quite obvious. As can be seen in Figure 10-a and b and also in Figure 10-c and d, the ferrite particles in hardened sample of diode laser are smaller than hardened sample of Nd:YAG laser, the cause of this effect is higher input energy and also higher absorption coefficient of diode laser compare to Nd:YAG laser (see section 3 and Table 4).

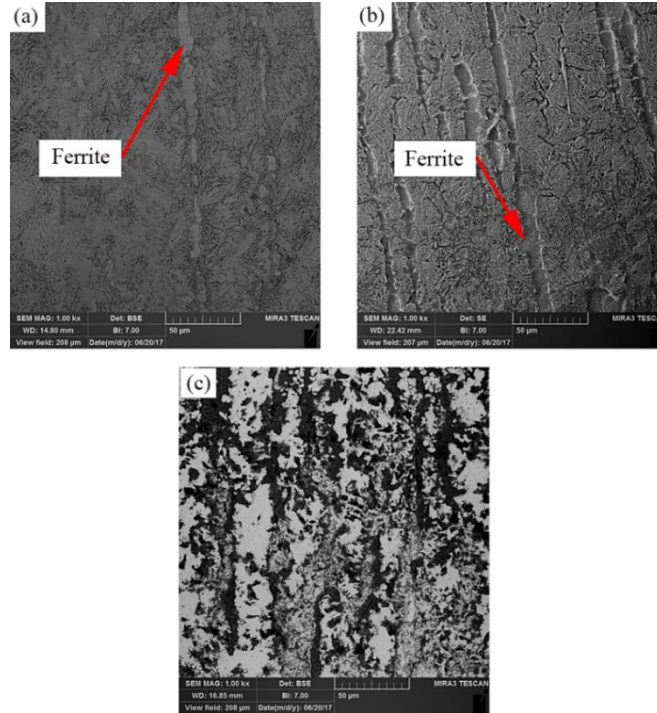


Figure 10. FESEM images of AISI 410 stainless steel a) microstructure of hardened layer by diode laser b) microstructure of hardened layer by Nd:YAG laser c) microstructure of the base metal

4-4 Micro hardness deviation from the base metal micro hardness (MHD)

The micro hardness deviation from base metal (MHD) is derived from Equation 5:

$$MHD = \sum_{i=1}^n \frac{(x_i - x_{b.m})^2}{n} \quad (5)$$

Where x_i is the micro hardness of different points, $x_{b.m}$ is the micro hardness of the base metal, and n is the number of points that their micro hardness is measured. In this paper n is, 10 and $x_{b.m}$ is equivalent to 330 Vickers (hardness of AISI 410). In laser hardening process the higher MHD is desired while a higher MHD value represents a more uniform hardness in the hardened area. Figure 11 shows the MHD in the depth and width of the hardened area by diode and Nd:YAG lasers.

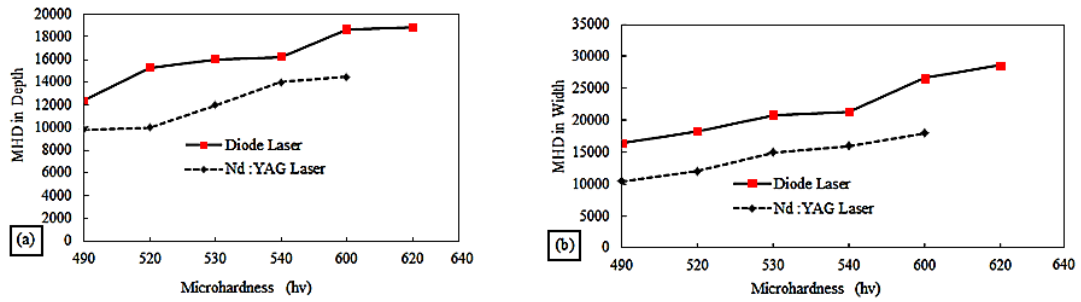


Figure 11. Diagram of Diode and Nd:YAG Laser of MHD a) in depth of hardened layer b) in width of hardened layer

It is deduced from Figure 11 that MHD value of the AISI 410 is increased with increasing hardness, which could be easily understand from Equation 5. The MHD of diode and the Nd:YAG lasers cases in Figure 11, a higher value and trend of MHD of both in depth and width in diode samples is seen.

4-5 The ferrite phase percentage in hardened layer

By analysis, the microstructure images of hardened area, the percentage of the ferrite phase particles in the field of martensite was evaluated by using Celemex software. It is deduced from Figure 12 that by increasing the hardness of AISI 410, the percentage of ferrite particles in the microstructure decreases. The level of the ferrite phase in Diode laser case is lower than the Nd:YAG laser case. The reason of this phenomenon is the higher input energy and also absorption coefficient in the diode laser than the Nd:YAG laser which increases the temperature of the steel austenite, so the most of the ferrite particles are dissolved in the microstructure at this temperature and their size becomes smaller.

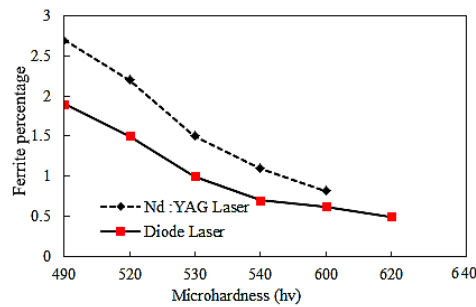


Figure 12. Diagram of ferrite particle in diode and Nd:YAG lasers

4-6 comparing the furnace hardening heat treatment and LSH

In this section, a comparative study on the analysis of the process and microstructure of the furnace hardening heat treatment and laser hardening by using two lasers, is presented. Cycle of furnace hardening heat treatment is shown in Fig. 13.

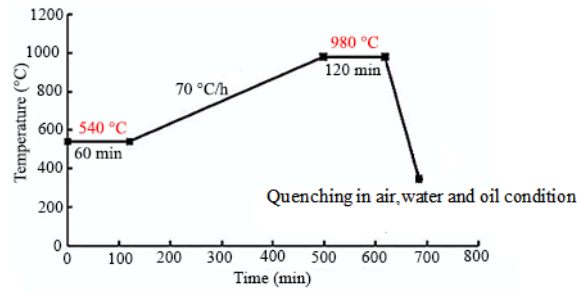


Figure 13. Cycle of Furnace hardening heat treatment of AISI 410 [37]

Cooling in oil condition, due to the lack of micro-cracking, is an ideal quenching. So the oil quenched sample with the hardness of 434 HV is selected as the best furnace heat treated conditions. Table 5 shows the comparison of furnace hardening heat treatment with diode and Nd:YAG laser hardening processes. As seen in Table 5 the hardness of the diode and Nd:YAG lasers are 1.43 and 1.37 times of furnace hardening, respectively.

Table 5. Comparison of furnace hardening heat treatment & LSH by diode and Nd:YAG lasers

Cycle of heat treatment	Furnace hardening heat treatment of AISI410	Diode Laser hardening	Nd:YAG Laser hardening
Quenching in oil	434 (h v)	-	-
Quenching in water	446 (h v)	-	-
Quenching in air	412 (h v)	-	-
Self-quenching by laser	-	620 (h v)	598 (h v)

As shown in Figure 14 in the furnace hardening heat treatment (Figure 14-a), fine-grained particles are distributed in the coarse martensitic field, and in diode LSH (Figure 14-b) the ferrites are fine particles and close together while in the Nd:YAG LSH (Figure 14-c), these particles are continuously interconnected. In LSH, due to the high energy concentration at the surface of the workpiece; hardening occurs locally, but the hardening in the furnace hardening heat treatment is volumetric.

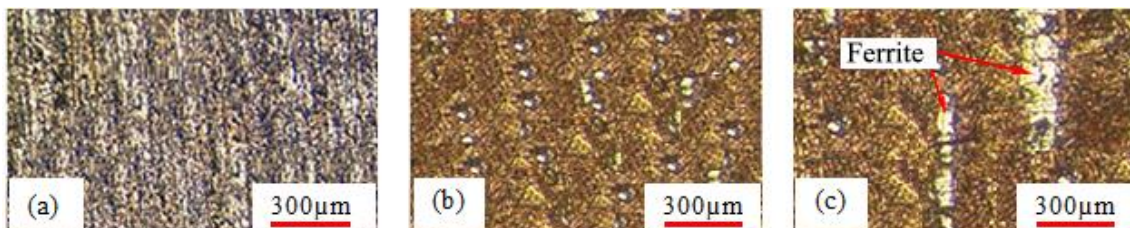


Figure 14. Microstructure images of a) furnace hardening heat treatment b) diode laser c) Nd:YAG laser

5- Conclusions

In this research, the effect of two types of laser; 1600 W high power diode laser and 700 W Nd:YAG laser on AISI 410 stainless steel was investigated. According to the experiments, the following results can be mentioned:

1. Each of the two type of lasers is suitable for AISI 410 LSH. However, due to the rectangular distribution energy of diode laser beam, if a greater amount of hardness is needed, a Diode laser can be used.

2. Higher microhardness deviation from the base material (MHD) in diode laser is achieved which make a more uniform hardening profile in hardened zone.
3. The maximum hardness value of AISI 410 obtained in diode laser hardening is 620 HV with 1.8 mm depth and in Nd:YAG laser hardening is 598 HV with 0.211 mm depth which are 1.43 and 1.37 times the hardness of furnace hardening heat treatment (434 Hv), respectively.
4. Ferrite particles in the furnace hardening samples are finer and distributed in the coarse martensitic field while in diode laser hardening microstructure are fine particles and close together and in Nd:YAG laser are continuously interconnected. In general, decreasing the percentage of the ferrite phase in the microstructure lead to increases the microhardness.

6- References

- [1] Leonard R. Migliore. Dekker: Laser materials processing, California; 1996.
- [2] Dieter Bäuerle. Springer: Laser Processing and Chemistry, Verlag Berlin Heidelberg; 2011.
- [3] R.A. Higgins. Engineering Metallurgy. Part 1: Applied Physical Metallurgy, 6th ed., Edward Arnold, London, 1993.
- [4] Laser Institute of America. Handbook of Laser Materials Processing, Magnolia Publishing Inc., 2001.
- [5] J. Grum. Comparison of different techniques of laser surface hardening. Journal of a achievements in Materials and Manufacturing Engineering 2007; 24 (1): 17-25.
- [6] A. H. Faraji, M. Moradi, M. Goodarzi, P. Coluccid, C. Maletta. An investigation on capability of hybrid Nd:YAG laser-TIG welding technology for AA2198 Al-Li alloy. Optics and Lasers in Engineering 2017; 96: 1-6.
- [7] M. Moradi, M. Ghoreishi, A. Rahmani. Numerical and Experimental Study of Geometrical Dimensions on Laser-TIG Hybrid Welding of Stainless Steel 1.4418. Journal of Modern Processes in Manufacturing and Production 2016; 5(2): 21-31.
- [8] J. Sundqvist, A. F. H. Kaplan, J. Granström, and K.G. Sundin. Identifying residual stresses in laser welds by fatigue crack growth acceleration measurement. Journal of Laser Applications 2015; 27.
- [9] Mahmoud Moradi, M Karami Moghadam, High Power Diode Laser Surface Hardening of AISI 4130; Statistical Modelling and Optimization, Optics and Laser Technology, 2019, 111, 554-570.
- [10] M Moradi, H Arabi, S Jamshidi Nasab, KY Benyounis. A comparative study of laser surface hardening of AISI 410 and 420 martensitic stainless steels by using diode laser. Optics and Laser Technology 2019; 111, 347-357.
- [11] M. Moradi, M. Ghoreishi and A. Khorram. Process and Outcome Comparison between Laser, Tungsten Inert Gas (TIG) and Laser-TIG Hybrid Welding. Journal of lasers in Engineering 2018; 39(6): 379-391.
- [12] M. Moradi, O. Mehrabi, T. Azdast, K. Y. Benyounis, Enhancement of low power CO₂ laser cutting process for injection molded polycarbonate, Optics & Laser Technology 2017; 96(06): 208–218.
- [13] Moradi M, Mohazabpak A. Statistical Modelling and Optimization of Laser Percussion Microdrilling of Inconel 718 Sheet Using Response Surface Methodology (RSM). Journal of lasers in Engineering 2018; 39(6): 313-331.
- [14] Mahmoud Moradi, Hadi Abdollahi. Statistical Modelling and Optimization of the Laser Percussion Microdrilling of Thin Sheet Stainless Steel. Journal of lasers in Engineering 2018; 40(6): 375-393.
- [15] F. Klocke, A. Demmer, A. Zaboklicki. Investigation into the use of high power diode lasers for hardening and thermal conduction welding. Proc. SPIE 3097 1997; 592–598.

- [16] M. Haag, T. Rudlaff. Assessment of different high power diode lasers for materials processing. Proc. SPIE 3097 1997; 583–591.
- [17] D.I. Pantelisa, E. Bouyiouria, N. Kouloumbib, P. Vassilioub, A. Koutsomichalisc. Wear and corrosion resistance of laser surface hardened structural steel. Surface and Coatings Technology 2002; (298): 125–134.
- [18] A.I. Katsamas, G.N. Haidemenopoulos, Surface hardening of low-alloy 15CrNi6 steel by CO₂ laser beam, Surface and Coatings Technology 1999; (115): 249–255.
- [19] P. Sun, Shaoxia Li, Gang Yu, Xiuli He, Caiyun Zheng and Weijian Ning. Laser surface hardening of 42CrMo cast steel for obtaining a wide and uniform hardened layer by shaped beams. Int J Adv Manuf Technol 2014 70: 787–796.
- [20] B. Ehlers, H.J. Herfurth, S. Heinemann. Hardening and welding with high power diode lasers. Proc. SPIE 3945 2000; 63–70.
- [21] M. Moradi, D. Ghorbani, M. Karami Moghadam, M. Kazazi, F. Rouzbahani, Sh. Karazie, Nd:YAG laser hardening of AISI 410 stainless steel: microstructural evaluation, mechanical properties, and corrosion behavior, Journal of Alloys and Compounds, 2019 795 (30): 213-222.
- [22] K. Benyounis, F. M. Shuaeib. An Indepth Investigation of Gas Nitriding of Stainless Steel: New DOE Parametric Studies and Optimization. Reference Module in Materials Science and Materials Engineering 2016; 1-12.
- [23] R. Li, Y. Jin, Zh. Li, & K. Qi, A Comparative Study of High-Power Diode Laser and CO₂ Laser Surface Hardening of AISI 1045 Steel, Journal of Materials Engineering and Performance 2014.VOL. 23,pp.3085–3091.
- [24] A. Fahdil iidan, O. Akimov, L.Golovco, O.Goncharuk, K.Kostyk, The study of the influence of laser hardening conditions on the change in properties of steel. Iadn 2016; 5(80).
- [25] Sh. Safdar, L. Li, M.A. Sheikh, M.J .Schmidt. Modelling the effect of laser beam geometry on laser surface heating of metallic materials. Proceedings of the 23 International Congress on Applications of Lasers and Electro-Optics 2004.
- [26] M. Moradi, H. Arabi. Experimental modeling of laser surface hardening process of AISI 410 by Response Surface Methodology. Modares Mechanical Engineering. 2018; 18(03): 179-188.
- [27] S.A. Jenabali Jahromi, A. Khajeh, B. Mahmoudi. Effect of different pre-heat treatment processes on the hardness of AISI 410 martensitic stainless steels surface-treated using pulsed neodymium-doped yttrium aluminum garnet laser. Materials and Design 2012; 34: 857–862.
- [28] R. E. Smallman, Modern physical Metallurgy, Furth Edition, Great Britain, The University of Birmengham, 1990.
- [29] Duley WW. Plenum: Laser Processing and Analysis of Materials, New York, 1983.
- [30] P.Molian, Surface modification technologies-An engineering guide TS Sudarshan (NewYork: Marcel 18, pp.14-31, 1989.
- [31] M. Moradi, M.M. Fallah, S. Jamshidi Nasab. Experimental study of surface hardening of AISI 420 martensitic stainless steel using high power diode laser. Transaction of the indian institute of metal: Springer Nature 2018; 71(8): 1-18.
- [32] M. Moradi, M. Arabi. Increasing the Surface Hardness of 410 Martensitic Stainless Steel Using High Power Diode Laser. Journal of Science and surface engineering 2018; (35): 59-70.
- [33] M. Moradi, M. KaramiMoghadam, J. Zarei, B. Ganji. The effects of gha laser pulse energy and focal point position on laser surface hardening of AISI 410 stainless steel. Modares Mechanical Engineering 2017; 17(7): 311-318.
- [34] M. Moradi, M. k. Moghadam, M Kazazi, Improved Laser Surface Hardening of AISI 4130 Low Alloy Steel with Electrophoretically Deposited Carbon Coating, Optik 2019; (178): 614-622.
- [35] B.Jung, H. Lee, H. Park. Effect of grain size on the indentation hardness for polycrystalline materials by the modified strain gradient theory. International Journal of Solids and Structures 2013; 50: 2719–2724.
- [36] X.Liu, F.Yuan, Y.Wei. Grain size effect on the hardness of nanocrystal measured by the nanosize indenter. Applied Surface Science 2013; 279: 159-166.
- [37] H. chandler. Heat Treater’s Guide, Practices and procedures for nonferrous alloys. The materials informat.